



BCL11B expression in intramembranous osteogenesis during murine craniofacial suture development

Greg Holmes ^{*}, Harm van Bakel, Xueyan Zhou, Bojan Losic, Ethylin Wang Jabs

Department of Genetics and Genomic Sciences, Icahn School of Medicine at Mount Sinai, New York, NY 10029, USA



ARTICLE INFO

Article history:

Received 24 October 2014

Received in revised form 26 November 2014

Accepted 3 December 2014

Available online 12 December 2014

Keywords:

Osteoblasts

Differentiation

Bone

Skull

Calvaria

Ctip2

ABSTRACT

Sutures, where neighboring craniofacial bones are separated by undifferentiated mesenchyme, are major growth sites during craniofacial development. Pathologic fusion of bones within sutures occurs in a wide variety of craniosynostosis conditions and can result in dysmorphic craniofacial growth and secondary neurologic deficits. Our knowledge of the genes involved in suture formation is poor. Here we describe the novel expression pattern of the BCL11B transcription factor protein during murine embryonic craniofacial bone formation. We examined BCL11B protein expression at E14.5, E16.5, and E18.5 in 14 major craniofacial sutures of C57BL/6J mice. We found BCL11B expression to be associated with all intramembranous craniofacial bones examined. The most striking aspects of BCL11B expression were its high levels in suture mesenchyme and increasingly complementary expression with RUNX2 in differentiating osteoblasts during development. BCL11B was also expressed in mesenchyme at the non-sutural edges of intramembranous bones. No expression was seen in osteoblasts involved in endochondral ossification of the cartilaginous cranial base. BCL11B is expressed to potentially regulate the transition of mesenchymal differentiation and suture formation within craniofacial intramembranous bone.

© 2014 Elsevier B.V. All rights reserved.

Proper growth of the skull requires the correct differentiation and coordinated growth of many individual bones. During development, the growing borders of neighboring bones are separated by undifferentiated mesenchyme in complexes called sutures. Premature obliteration of these sutures by the inappropriate fusion of adjacent bones and loss of the intervening mesenchyme occurs in craniosynostosis, involving calvarial sutures (Morris-Kay and Wilkie, 2005). Facial sutures may also be affected, causing midface retrusion, which can occur with craniosynostosis or independently (Kreiborg, 2000). The list of genes in which mutations result in suture fusion in both humans and mice is growing, particularly for syndromic craniosynostosis, but the genetic basis for the majority of human craniosynostosis, which is non-syndromic, is still largely unknown (Heuzé et al., 2014; Holmes, 2012; Jabs and Lewanda, 2013; Wilkie et al., 2010). A complete knowledge of gene expression within the osteogenic fronts and suture mesenchyme will aid the discovery of such genes, and enhance our understanding of suture biology and craniofacial growth.

BCL11B (also known as COUP-TF interacting protein 2 or CTIP2) is a Kruppel-like C2H2 transcription factor (Avram et al., 2000). BCL11B can interact with COUP-TF or HDACs and other chromatin-associated proteins to repress transcription (Avram et al., 2000; Marban et al., 2007). Transcriptional targets of BCL11B include cell cycle regulators (Cherrier et al., 2009; Topark-Ngarm et al., 2006) and signaling pathways affected include those of FGF, SHH, EGF, and NOTCH (Kyrylkova et al., 2012; Zhang et al., 2012). During embryonic development, BCL11B is expressed in the brain, thymus, skin epidermis, dermis, and hair follicles, oral and gut epithelia, and teeth (Arlotta et al., 2005; Golonzka et al., 2007, 2009b; Leid et al., 2004). Total and conditional mouse knockouts of *Bcl11b* have revealed its critical role in the development of thymocytes (Wakabayashi et al., 2003), neurons (Arlotta et al., 2005), skin (Golonzka et al., 2009a) and teeth (Golonzka et al., 2009b). While BCL11B expression in early facial mesenchyme has also previously been shown (Chan et al., 2007; Leid et al., 2004), an observation of midfacial hypoplasia in *Bcl11b* knockout mice has only recently been described (Golonzka et al., 2009b; Katsuragi et al., 2013), and an understanding of how the known BCL11B expression domains could relate to this phenotype is lacking. Here, we show that BCL11B is widely expressed during suture development in murine embryos, and describe its expression patterns across a comprehensive range of craniofacial sutures that have not previously been shown to express BCL11B. Its ubiquitous presence at these sites suggests an important role for BCL11B in the regulation of osteogenic differentiation and suture formation.

* Corresponding author. Department of Genetics and Genomic Sciences, Icahn School of Medicine at Mount Sinai, One Gustave L. Levy Place, 1428 Madison Avenue, New York, NY, 10029, USA. Tel.: +1 212 659 1529; fax: +1 212 241 7112.

E-mail address: gregory.holmes@mssm.edu (G. Holmes).

1. Results

It is known that *Bcl11b* is diffusely expressed in the distal mandibular and facial mesenchyme during early embryogenesis, including murine embryonic day (E) 12.5 (Chan et al., 2007; Leid et al., 2004). We used an established antibody to BCL11B (Arlotta et al., 2005; Kyrylkova et al., 2012; Senawong et al., 2003; Topark-Ngarm et al., 2006) to determine the relationship between BCL11B expression and craniofacial bone formation during embryonic mouse development, starting at E14.5, when most craniofacial bones have begun to form. Embryonic heads were sectioned in the sagittal, coronal and transverse planes to study 14 different sutures and their associated bones. To better define when BCL11B is expressed during osteogenesis, sections were co-immunostained with a RUNX2 antibody that identifies committed osteoprogenitors and mature osteoblasts.

1.1. Craniofacial expression of BCL11B at E14.5

At E14.5, the BCL11B protein was widely detected throughout the facial mesenchyme, and co-expressed with RUNX2 in osteogenic regions, with the exception of more differentiated osteoblasts (Table 1). Specifically, BCL11B expression overlapped with RUNX2 in osteogenic mesenchyme encompassing the premaxillary, maxillary and palatine bones, and the presumptive suture mesenchyme. However, BCL11B was absent in the more mature osteoblasts at the core of these elements, indicated by areas of matrix deposition or increased intensity of RUNX2 expression (Fig. 1A–D).

In the vomer bones of the nasal septum BCL11B was expressed within the domain of RUNX2 expression, particularly ventrally and in the outer domain of RUNX2 (Fig. 2A, B). BCL11B was expressed in the lateral and medial peripheries of the maxillary bone, and in the RUNX2-positive condensing mesenchyme adjacent to the medial epithelial seam of the fusing palatal shelves (Fig. 2C, D). BCL11B was co-expressed with RUNX2 throughout both the nasal bone anlagen and presumptive internasal suture mesenchyme (Fig. 2F). In the calvarial interparietal bone, BCL11B expression overlapped with RUNX2 expression, but the highest expression was confined to the periphery of the bone anlagen (Fig. 1F). At the ventral edge of the calvarial frontal bone, BCL11B expression was restricted to the peripheral area of lower RUNX2 expression (Fig. 2G).

The areas where BCL11B expression was present in the absence of RUNX2 include the facial mesenchyme anterior to the premaxillary and mandibular bones (Fig. 1A, B, E). The anterior palatal shelf mesenchyme lacked BCL11B and RUNX2 expression,

apart from a few BCL11B-positive cells adjacent to the medial palatal epithelium (Fig. 2E). In contrast to the facial bones, RUNX2-positive cells of the mandibular bone and the adjacent BCL11B-positive mesenchyme showed only a narrow area of overlap (Fig. 1E). BCL11B was absent from the cartilage of the nasal septum and turbinates (Figs. 1B, 2B, F), cranial base, and inner ear (not shown).

1.2. Craniofacial expression of BCL11B at E16.5

At E16.5 BCL11B expression was still present in the distal facial mesenchyme (Fig. 3A, B). Compared to E14.5 the relationship between BCL11B expression and osteogenesis was more sharply defined and overlapped less with RUNX2, as exemplified by expression associated with the nasal bone and adjacent frontal and premaxillary bones. Mesenchymal BCL11B expression surrounded the RUNX2-positive nasal bone, partially overlapping with less intensely RUNX2-positive cells in a layer of only a few cells thickness (Fig. 3A, C). Expression continued posteriorly throughout the mesenchyme of the presumptive frontonasal suture, which expressed low levels of RUNX2, and anteriorly into the mesenchyme of the nasopremaxillary suture, which lacked RUNX2. Unlike the broad co-expression seen in this suture at E14.5, the overlap between sutural BCL11B and premaxillary RUNX2 expression typically consisted of a single cell layer. BCL11B was distinctly expressed in the mesenchyme of the premaxillary/maxillary and maxillary/palatine sutures, and in the mesenchyme surrounding the posterior edge of the palatine bone. BCL11B expression extended along the bone surfaces away from suture mesenchyme but was typically confined to one or two cell layers, or not detectable (Fig. 3D–F). High BCL11B expression extended anteroposteriorly and mediolaterally throughout the overlapping maxillary/palatine suture (Figs. 3E, 4A, B). In contrast, expression in the midline interpalatine (Fig. 4C) and intermaxillary (not shown) sutures was low, with increased expression confined to the mesenchyme at the medial periphery of the palatine and maxillary bones, while RUNX2 expression extended across the midline suture mesenchyme. Peripheral mesenchyme surrounding the vertical extensions of the palatine bones also expressed BCL11B (Fig. 4D). In calvarial bones such as the frontal bone, BCL11B continued to be expressed along their outer margins (Fig. 4E). Another distinctive site of high BCL11B expression could now be found in the RUNX2-negative suture mesenchyme between the zygoma (jugal bone) and zygomatic process of the maxillary bone in the maxillary/zygomatic suture, and showed some overlap with the outer layers of RUNX2-positive osteoblasts (Fig. 4F). Expression was also seen in the molar epithelium and restricted regions of the adjacent mesenchyme, as previously reported (Fig. 4G) (Golonzha et al., 2009b). BCL11B expression was not detected in association with mandibular bone (not shown). Within the cranial base, BCL11B expression was absent from cartilage and sites of endochondral ossification where RUNX2-positive osteoblasts were present in the perichondrium and on trabeculae (not shown).

BCL11B expression was also examined in the calvarial sutures at E16.5. In both the sagittal and interfrontal sutures the parietal and frontal bone edges, respectively, are widely separated by mesenchyme. BCL11B was co-expressed with RUNX2 in the less mature osteogenic mesenchyme at their peripheries but excluded from more differentiated osteoblasts adjacent to osteoid (Fig. 5A, B). In the coronal suture, the frontal and parietal bone edges are typically overlapping and RUNX2 expression is more tightly confined to the bone edges. BCL11B expression was strongest in RUNX2-negative cells of the suture mesenchyme and only overlapped narrowly with RUNX2-positive cells (Fig. 5C). In the squamoparietal suture, BCL11B was expressed most strongly in the suture mesenchyme, where RUNX2 expression was low (Fig. 5D).

Table 1

Relative BCL11B expression in major craniofacial sutures during embryonic murine development^a.

Suture	E14.5	E16.5	E18.5
Frontonasal	++	++	++
Nasopremaxillary	++	++	+++
Premaxillary/maxillary	++	++	+++
Maxillary/palatine	++	+++	+++
Internasal	++	++	+++
Interpremaxillary	na	+	+
Intermaxillary	na	+	+
Interpalatine	na	+	+
Maxillary/zygomatic	na	+++	++
Squamoparietal	na	+	++
Interfrontal	na	++	+
Sagittal	na	++	+
Coronal	+	++	++
Lambdoid	na	++	+

^a Expression key: +, weak; ++, medium; +++, strong; na, not applicable (suture absent or not obvious). See text for distribution of expression within sutures.

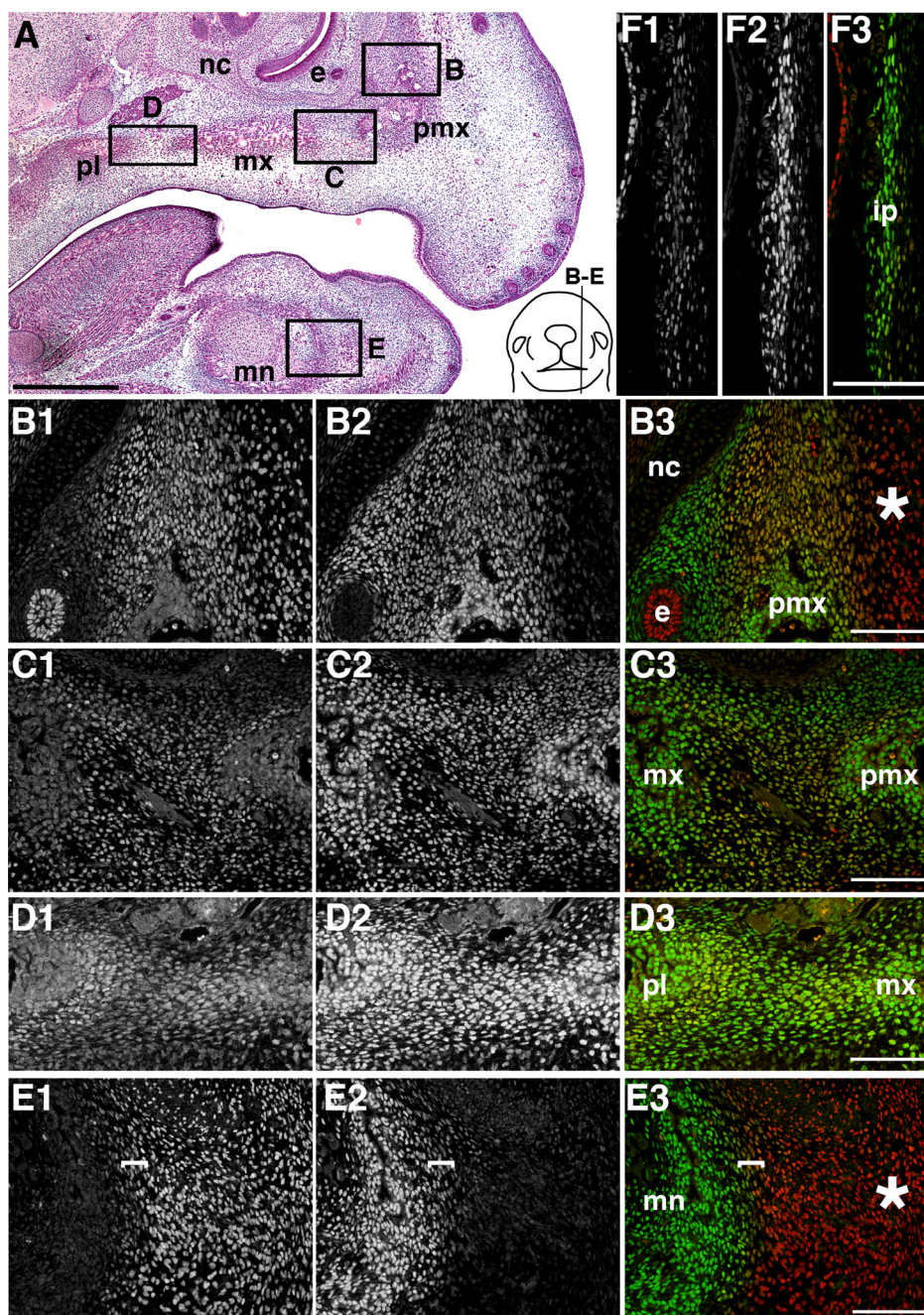


Fig. 1. Craniofacial BCL11B expression at E14.5 compared with RUNX2 (sagittal plane). (A) Hematoxylin and eosin (HE) staining of a parasagittal section indicating boxed areas immunostained in B–E. The location of the section is shown on the inset schematic. (B–F) Co-immunostaining results for BCL11B (B1–F1) and RUNX2 (B2–F2) are shown separately as gray channel images, or merged (B3–F3; red, BCL11B; green, RUNX2). (B) Premaxillary bone. Asterisk indicates BCL11B-positive/RUNX2-negative facial mesenchyme. (C) Premaxillary/maxillary suture. (D) Maxillary/palatine suture. (E) Mandible and adjacent anterior mesenchyme. Brackets indicate narrow overlap of BCL11B and RUNX2 expression. Asterisk indicates BCL11B-positive/RUNX2-negative mesenchyme. (F) Interparietal bone. Scale bars: 500 μ m for A and 100 μ m for B–F. Abbreviations: e, tangential section of nasal epithelium; ip, interparietal bone; mn, mandible; mx, maxillary bone; nc, nasal cartilage; pl, palatine bone; pmx, premaxillary bone.

1.3. Craniofacial expression of BCL11B at E18.5

Craniofacial expression of BCL11B at E18.5 was similar to that at E16.5 (Table 1). In the facial sutures the strongest expression remained within the maxillary/palatine suture mesenchyme, and was also distinct within the suture mesenchyme between frontal, nasal and premaxillary bones (Fig. 6A–D). In contrast to the sparse BCL11B expression generally seen along bone surfaces away from the suture, the premaxillary bones were surrounded by a two-to-three cell layer of BCL11B-positive/RUNX2-negative cells (Fig. 6A, B). Interpalatine

and intermaxillary BCL11B suture expression remained confined along the bone edges within the suture, except where the suture was narrowest and expression was in the central mesenchyme (not shown). In the cranium BCL11B was most strongly expressed in the coronal and squamoparietal suture mesenchyme (Fig. 6E; Table 1). In the posterior interfrontal, sagittal and lambdoid sutures, where adjacent bone edges were more widely separated, BCL11B expression extended from the peripheral edges of interfrontal, parietal and interparietal bones, overlapping with low RUNX2 expression as at E16.5. In the anterior interfrontal suture low levels of BCL11B and

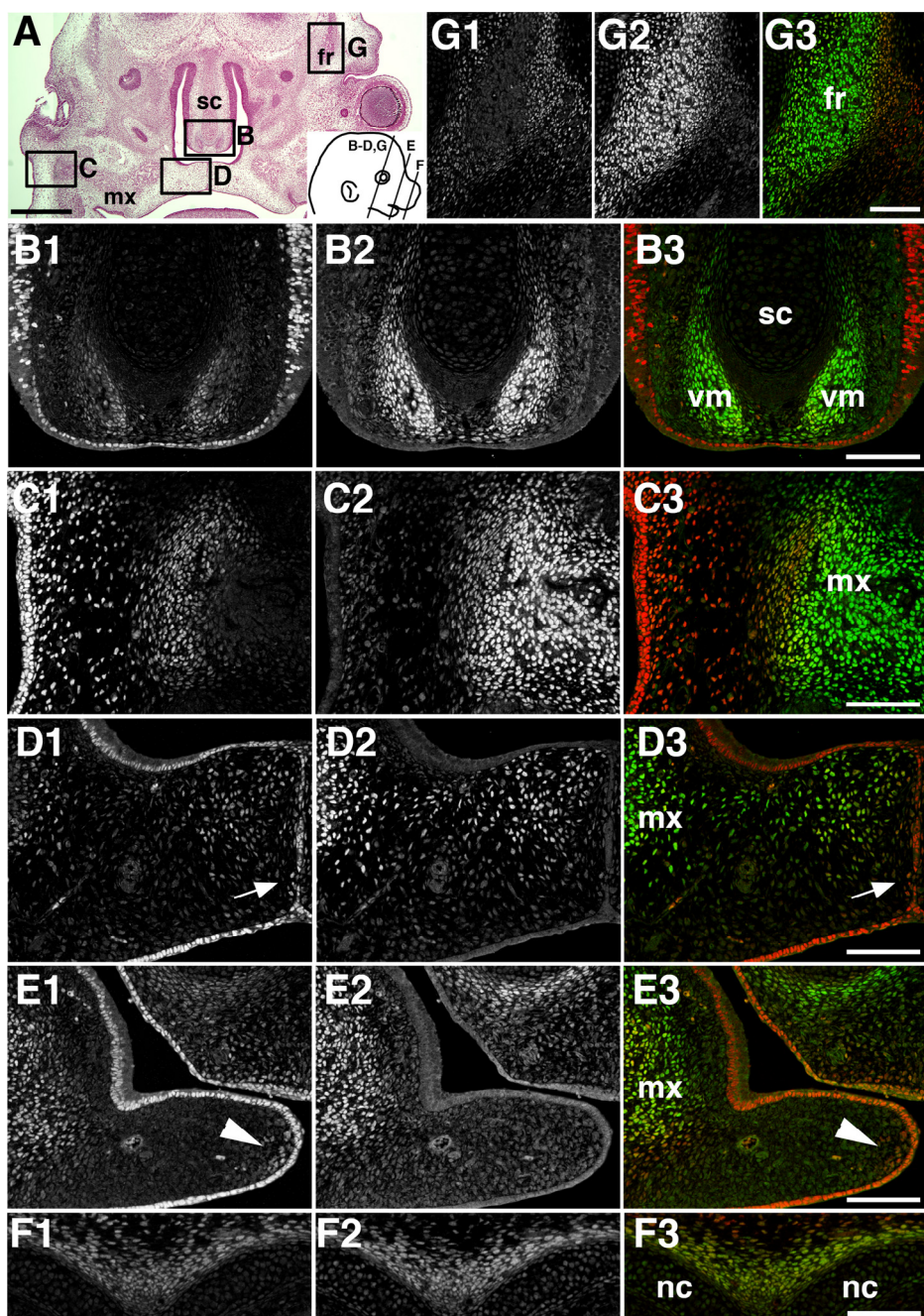


Fig. 2. Craniofacial BCL11B expression at E14.5 compared with RUNX2 (coronal plane). (A) HE staining of a coronal section indicating boxed areas immunostained in B, C, D, G. The location of this section and that of E and F is shown on the inset schematic. (B–G) Co-immunostaining results for BCL11B (B1–G1) and RUNX2 (B2–G2) are shown separately as gray channel images, or merged (B3–G3; red, BCL11B; green, RUNX2). (B) Vomer bones. (C) Lateral edge of the maxillary bone. (D) Medial edge of the maxillary bone and mid-palatal mesenchyme. Arrow indicates medial epithelial seam. (E) Medial edge of the maxillary bone and palatal mesenchyme anterior to plane of section in A (see inset schematic). Arrowhead indicates BCL11B-positive palatal mesenchyme cells. (F) Nasal bone anlagen and internasal suture mesenchyme anterior to plane of section in A (see inset schematic). (G) Ventral edge of frontal bone. Scale bars: 500 µm for A and 100 µm for B–G. Abbreviations: fr, frontal bone; mx, maxillary bone; nc, nasal cartilage; sc, septal cartilage; vm, vomer bone.

RUNX2 could now be seen throughout the suture mesenchyme (Fig. 6F).

1.4. Co-expression of BCL11B and other osteoblast markers

We further delineated the relationship between BCL11B and osteogenesis by comparing its expression to that of alkaline phosphatase (ALP) activity, which is upregulated in preosteoblasts (Candelier et al., 2001). Typically, BCL11B expression was excluded from regions of increased ALP activity, coinciding with

increased RUNX2 expression, as seen in the coronal, maxillary/palatine and maxillary/zygomatic sutures at E16.5 (Fig. 7A–F). Overlap of BCL11B expression and high ALP activity, as shown in the sutural surface of the zygomatic process of the maxillary bone within the maxillary/zygomatic suture, was rarely seen (Fig. 7E).

The DNA-binding protein SATB2 is expressed in the cerebral cortex, early craniofacial mesenchyme, and differentiated bone (Dobreva et al., 2006; Szemes et al., 2006). In differentiating neurons of the cortex, SATB2 directly downregulates *Bcl11b* expression (Alcamo et al., 2008). To determine whether a similar relationship

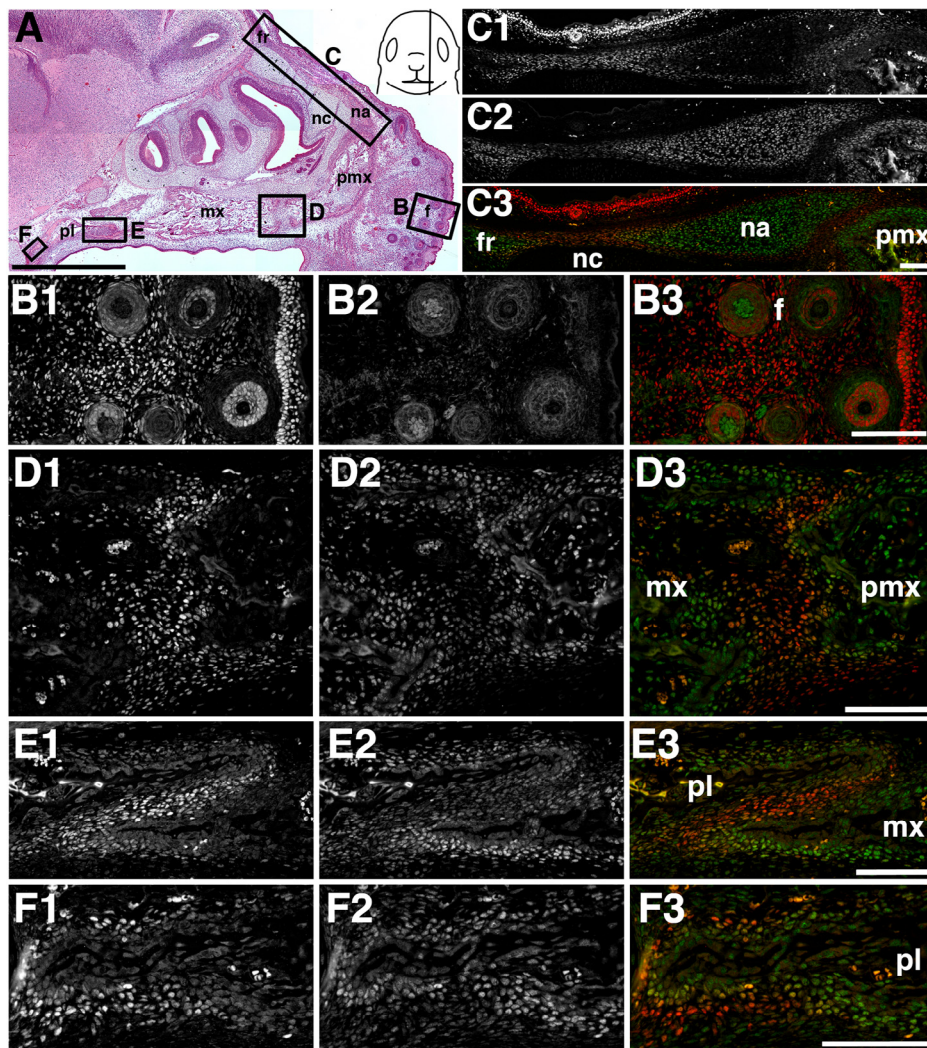


Fig. 3. Craniofacial BCL11B expression at E16.5 compared with RUNX2 (sagittal plane). (A) HE staining of a parasagittal section indicating boxed areas immunostained in B–F. The location of the section is shown in the inset schematic. (B–F) Co-immunostaining results for BCL11B (B1–F1) and RUNX2 (B2–F2) are shown separately as gray channel images, or merged (B3–F3; red, BCL11B; green, RUNX2). (B) Facial mesenchyme and whisker follicles. (C) Nasal bone, adjacent frontal and premaxillary bones, and intervening sutures. (D) Premaxillary/maxillary suture. (E) Maxillary/palatine suture. (F) Posterior edge of palatine bone. Scale bars: 1 mm for A and 100 μ m for B–F. Abbreviations: f, whisker follicles; fr, frontal bone; mx, maxillary bone; na, nasal bone; nc, nasal cartilage; pl, palatine bone; pmx, premaxillary bone.

may be possible during bone formation, we co-immunostained sections as before at E14.5, E16.5 and E18.5 for BCL11B and SATB2 expression. SATB2 expression was confined to mature osteoblasts adjacent to secreted osteoid, and was typically not adjacent to cells expressing BCL11B, suggesting that SATB2 may not be involved in *Bcl11b* downregulation in osteoblasts (Fig. 8).

In the neural cortex the major population of BCL11B-positive cells is post-mitotic, but BCL11B is expressed in proliferating oral epithelial cells (Arlova et al., 2005; Golonzka et al., 2007). We co-immunostained sections at E14.5 and E16.5 for BCL11B and Ki67, a marker for proliferating cells, and found no specific exclusion of BCL11B from proliferating cells within areas of suture or bone formation (not shown).

1.5. Expression of *Bcl11b* and other genes in the coronal suture at E16.5

We confirmed mRNA expression of *Bcl11b* in the coronal suture and compared its level of expression to that of *Runx2* and other genes of the suture complex. By using RNA-Seq analysis of mRNA derived from four independent microdissected coronal suture prepara-

tions, we observed that *Bcl11b* was clearly expressed above background levels of gene expression, though lower than other known sutural genes, such as *Twist1*, *Fgfr2*, *Runx2*, and *Sp7* (*Osterix*) (Fig. 9).

2. Discussion

While the existence of *Bcl11b* expression in the early facial mesenchyme was previously known (Chan et al., 2007; Leid et al., 2004), the recent demonstrations of midfacial hypoplasia in *Bcl11b*^{-/-} mice suggest a later role for this transcription factor in craniofacial development (Golonzka et al., 2009b; Katsuragi et al., 2013). Indeed, we have found BCL11B expression to be intimately associated with suture formation and osteoblast differentiation during intramembranous craniofacial bone development.

By E14.5 formation of all major craniofacial bone anlagen has begun. BCL11B expression is extensive in both anterior facial and mandibular non-osteogenic mesenchyme, and in the mesenchyme surrounding and separating the premaxillary, maxillary and palatine bones. These bones form within a broad region of RUNX2 expression that includes the presumptive suture mesenchyme, and

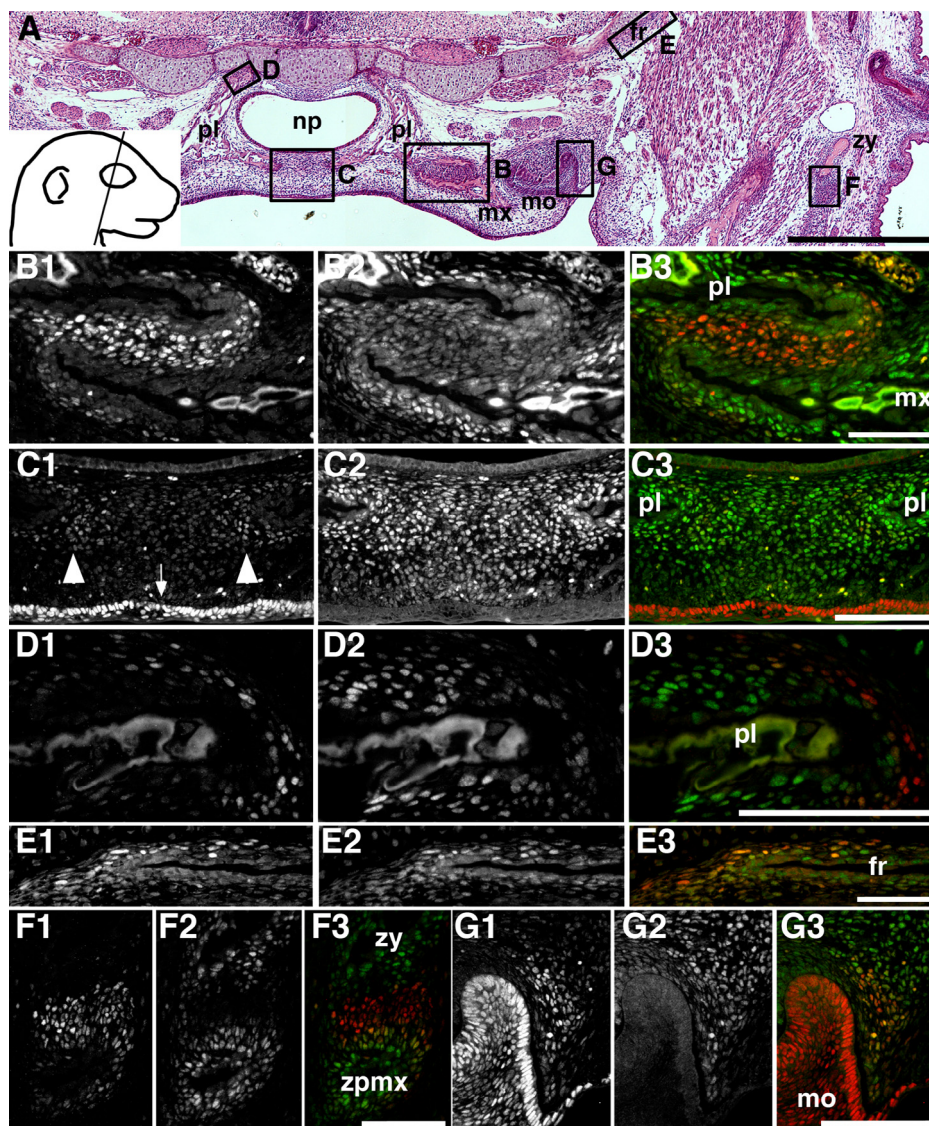


Fig. 4. Craniofacial BCL11B expression at E16.5 compared with RUNX2 (coronal plane). (A) HE staining of a coronal section indicating boxed areas immunostained in B–G. The location of the section is shown on the inset schematic. (B–G) Co-immunostaining results for BCL11B (B1–G1) and RUNX2 (B2–G2) are shown separately as gray channel images, or merged (B3–G3; red, BCL11B; green, RUNX2). (B) Maxillary/palatine suture. (C) Interpalatine suture. Arrowheads and arrow in C1 indicate domains of relatively higher BCL11B expression peripheral to the palatine bones and strong expression in the palatal epithelium, respectively. (D) Dorsal edge of palatine bone. (E) Ventral edge of frontal bone. (F) Zygomatic/maxillary suture. (G) Molar. Scale bars: 500 μ m for A and 100 μ m for B–G. Abbreviations: fr, frontal bone; mo, molar; mx, maxillary bone; pl, palatine bone; np, nasopharynx; zpmx, zygomatic process of maxillary bone; zy, zygoma.

so BCL11B and RUNX2 expression overlap extensively. Co-expression in the calvarial bone anlagen was also seen at E14.5. However, BCL11B expression is clearly downregulated in more differentiated osteoblasts. As development proceeds, the expression of BCL11B becomes more sharply defined. By E16.5 the most distinct BCL11B expression is seen in suture mesenchyme where RUNX2 expression is low or absent, especially within the maxillary/palatine and maxillary/zygomatic sutures. A notable exception to this pattern is seen in the interpalatine and intermaxillary sutures at E16.5, where higher BCL11B expression is confined to the medial perimeters of the palatine and maxillary bones and is low in the intervening RUNX2-positive suture mesenchyme. These trends continue at E18.5. While BCL11B expression can coincide with low levels of RUNX2, it generally becomes sharply attenuated with increased RUNX2 expression within differentiating osteoblasts. This exclusion of BCL11B from differentiating osteoblasts is also evident in the mutually exclusive expression of BCL11B and ALP generally seen during bone

formation. BCL11B expression can also extend along the flat bone surfaces within one or two cell layers, where expression includes RUNX2-negative cells, and can be significantly expressed at the non-sutural edges of bone. Interestingly, BCL11B expression was not detected in osteoblasts involved in endochondral ossification in the skull.

Skeletal elements initiate as mesenchymal condensations whose cells differentiate to chondrogenic or osteoblastic fates (Hall and Miyake, 2000). Through ill-defined mechanisms these condensations eventually end mesenchymal cell recruitment and expand by autonomous growth as discreet skeletal elements. Similarly, the molecular mechanisms governing the formation and maintenance of the sutures separating the intramembranous bones of the skull are poorly understood. Most of our knowledge comes from the more intensively studied calvarial sutures such as the coronal, sagittal and interfrontal, with little known about these processes in facial sutures (Depew et al., 2008; Di Ieva et al., 2013; Holmes, 2012; Morris-Kay

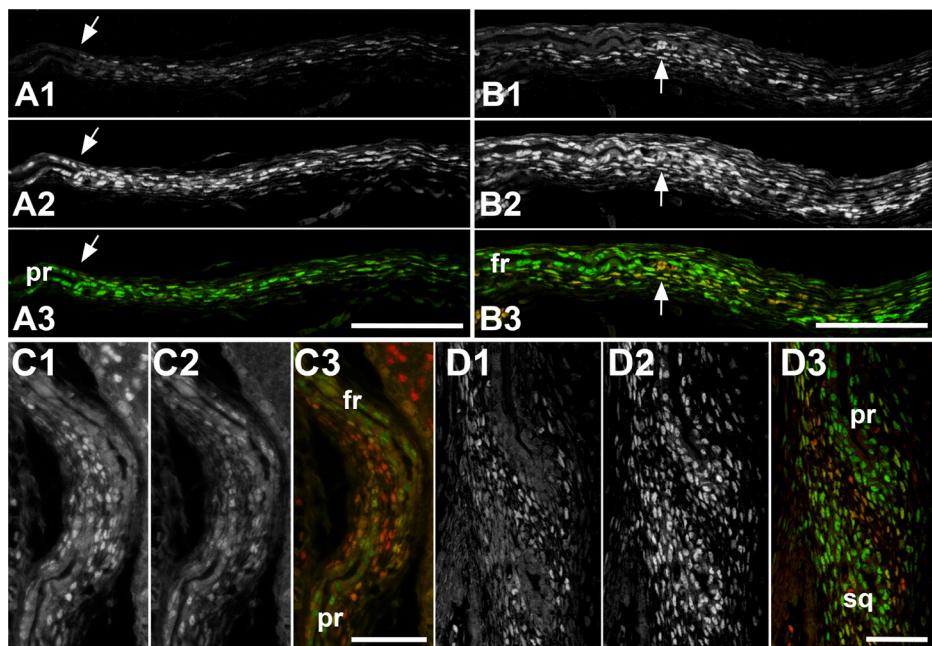


Fig. 5. Calvarial suture expression of BCL11B at E16.5 compared with RUNX2. (A–D) Co-immunostaining results for BCL11B (A1–D1) and RUNX2 (A2–D2) are shown separately as gray channel images, or merged (A3–B3; red, BCL11B; green, RUNX2). (A) Coronal section of sagittal suture adjacent to parietal bone. Arrow indicates the parietal osteoid edge. (B) Coronal section of interfrontal suture adjacent to frontal bone. Arrow indicates the frontal osteoid edge. (C) Transverse section of coronal suture. (D) Coronal section of squamoparietal suture. Scale bars: 100 µm for A, B and 50 µm for C, D. Abbreviations: fr, frontal bone; pr, parietal bone; sq, squamosal bone.

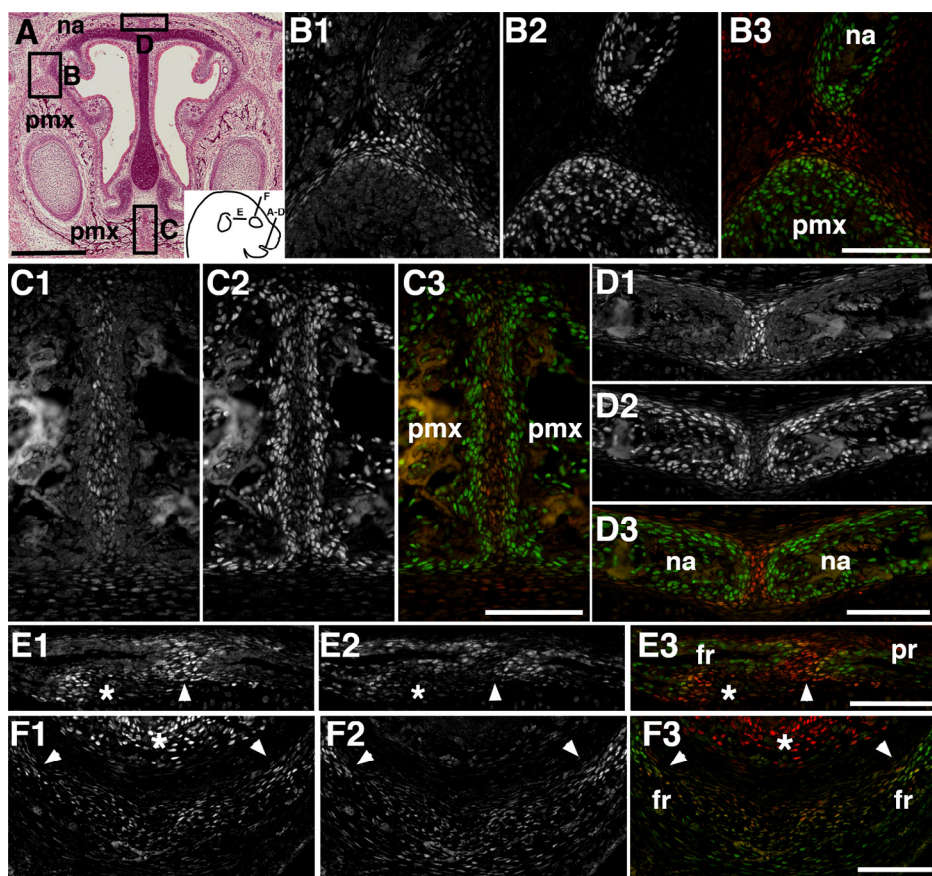


Fig. 6. Craniofacial BCL11B expression at E18.5 compared with RUNX2. (A) HE staining of an anterior coronal section indicating boxed areas immunostained in B–D. The location of the section is shown on the inset schematic. (B–F) Co-immunostaining results for BCL11B (B1–F1) and RUNX2 (B2–F2) are shown separately as gray channel images, or merged (B3–F3; red, BCL11B; green, RUNX2). (B) Nasopremaxillary suture. (C) Interpremaxillary suture. (D) Internasal suture. Compare to Fig. 2F. (E) Transverse section of the coronal suture (inferior level; see inset schematic). Note expression of BCL11B in suture mesenchyme between the frontal and parietal bones (arrowhead) and additional expression at the inner table edge of the frontal bone at this level (asterisk). (F) Coronal section of the interfrontal suture (see inset schematic). Arrowheads indicate medial edges of frontal bones; asterisk indicates epithelial BCL11B expression. Scale bars: 500 µm for A and 100 µm for B–F. Abbreviations: fr, frontal bone; na, nasal bone; pmx, premaxillary bone; pr, parietal bone.

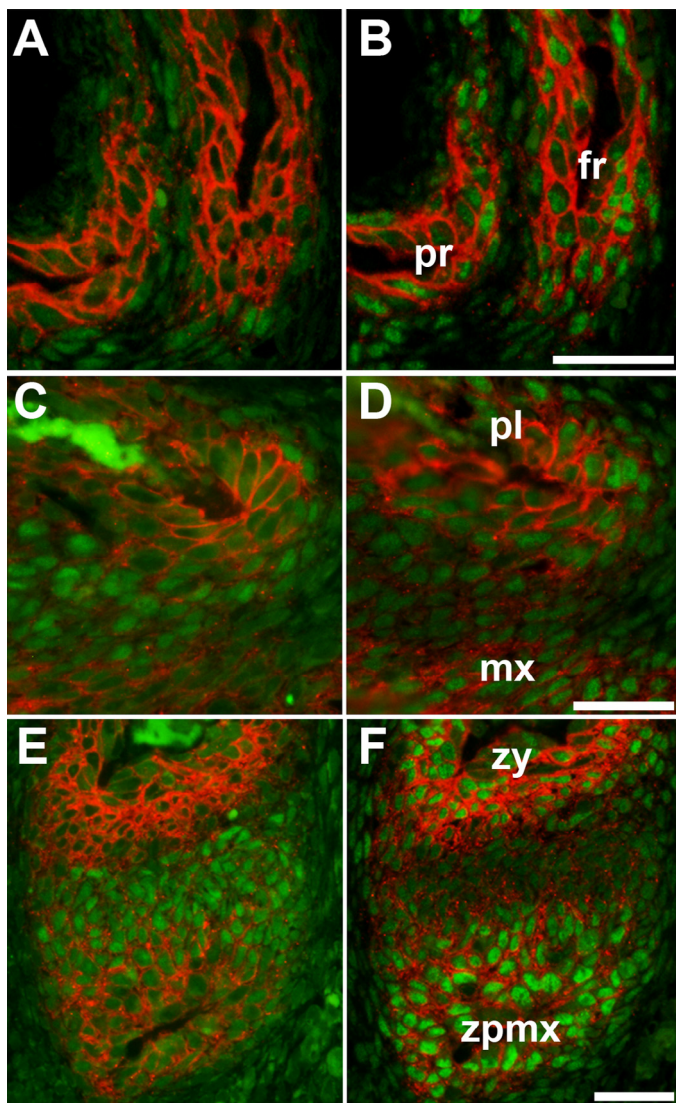


Fig. 7. Comparison of BCL11B and RUNX2 protein expression with ALP activity within craniofacial sutures at E16.5. Histochemical staining for ALP (red) was combined with immunostaining for BCL11B (A, C, E) or RUNX2 (B, D, F) (green) in (A, B) transverse sections of the coronal suture. (C, D) Coronal sections of the maxillary/palatine suture (lateral edge shown). (E, F) Coronal sections of the zygomatic/maxillary suture. Scale bars: 100 μ m. Abbreviations: fr, frontal bone; mx, maxillary bone; pl, palatine bone; pr, parietal bone; zpmx, zygomatic process of maxillary bone; zy, zygoma.

and Wilkie, 2005; Opperman, 2000). Impediments to this understanding are our general ignorance of gene expression across all sutures and of the origins of suture mesenchyme. In the calvaria, the coronal suture originates from a specific population of apically-migrating mesoderm cells between E11 and E13 (Deckelbaum et al., 2012). The sagittal suture is composed of mesoderm-derived cells posteriorly and neural crest-derived cells anteriorly, while the interfrontal suture is neural crest-derived, but the more immediate origins of these populations are not known (Jiang et al., 2002; Yoshida et al., 2008). A major question in calvarial bone growth is the extent to which the bones enlarge by autonomous growth or by incorporation of adjacent cells from the presumptive sutural mesenchyme. Current evidence suggests that growth is largely autonomous, with minor incorporation of adjacent presumptive suture mesenchyme but exclusion of the cells from the definitive suture mesenchyme (Lana-Elola et al., 2007; Ting et al., 2009; Yoshida et al., 2008). TWIST1 and its interacting proteins provide a major mechanism maintaining suture mesenchyme and regulating osteogenesis at the osteogenic

fronts (Connerney et al., 2006, 2008; Merrill et al., 2006; Sharma et al., 2013; Ting et al., 2009; Yen et al., 2010). We found that BCL11B was expressed within the calvarial bone anlagen at E14.5, but also extended into RUNX2-negative peripheral mesenchyme, raising the possibility that BCL11B may be involved in defining the mesenchymal condensation.

The origin of facial suture mesenchyme, derived from the neural crest like the facial bones, is also unclear. That the premaxillary, maxillary and interpalatine bones and their intervening suture mesenchymes initially form within a common domain of RUNX2 expression suggests mechanisms to repress RUNX2-mediated osteogenesis within the presumptive suture mesenchyme in addition to suture formation. BCL11B expression is localized to potentially be involved in this function, or at least to regulate or shape the transition of mesenchymal cells to osteoblasts. HDAC activity and cell cycle regulation are important determinants of craniofacial bone development (Bradley et al., 2011; Hall et al., 2014; Miller et al., 2010), and are potential avenues of BCL11B function (Cherrier et al., 2009; Marban et al., 2007; Topark-Ngarm et al., 2006). These potential roles are compatible with its expression along bone surfaces and at the

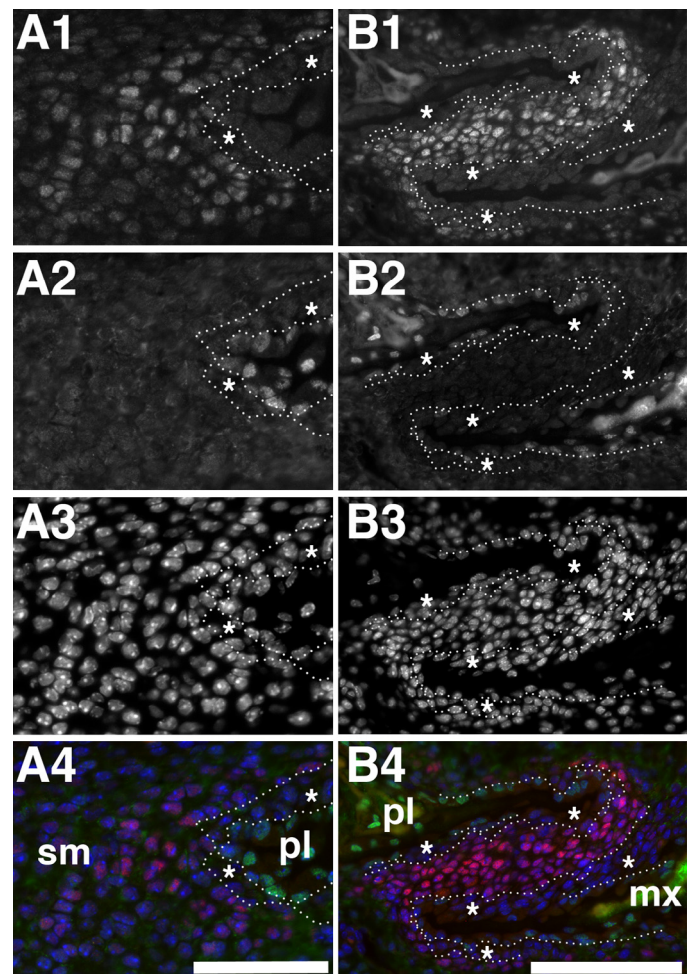


Fig. 8. Comparison of BCL11B and SATB2 protein expression within craniofacial sutures at E16.5 (coronal plane). A, B: Co-immunostaining results for BCL11B (A1, B1), SATB2 (A2, B2), and Hoechst 33258 (nuclei; A3, B3) are shown separately as gray channel images, or merged (A4, B4; red, BCL11B; green, SATB2; blue, Hoechst 33258). A: One edge of the interpalatine suture. B: Maxillary/palatine suture. Dotted lines overlaid in each panel delineate the edges of BCL11B and SATB2 expression. Asterisks indicate sutureal cells negative for both BCL11B and SATB2 expression. Scale bars: 50 μ m for A and 100 μ m for B. Abbreviations: mx, maxillary bone; pl, palatine bone; sm, suture mesenchyme.

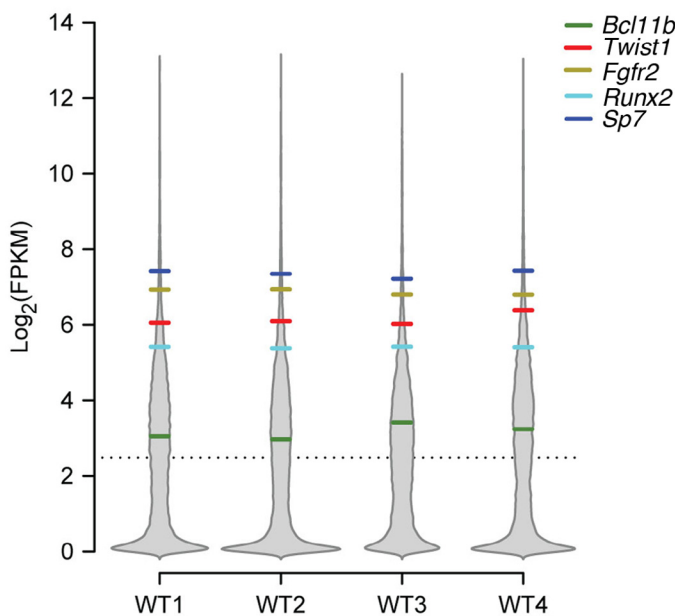


Fig. 9. Relative expression of *Bcl11b* and other osteogenic markers in the coronal suture at E16.5. Gene expression in four independent, wild-type (WT1–4) coronal suture preparations is shown as log₂ FPKM (Fragments Per Kb of transcript per Million reads). The background distribution of expression levels for all other expressed genes is shown as a violin plot (gray) for comparison, in which the relative width of the shape corresponds to the density of genes at any given FPKM level. The dashed line corresponds to the average gene expression level across all 4 samples.

non-sutural edges of bones such as the palatine and maxillary bones. The creation of a mouse expressing Cre-ERT under control of the *Bcl11b* promoter (or the promoters of other genes expressed in suture mesenchyme) would provide an invaluable tool for investigating the dynamics of mesenchymal recruitment into skeletal condensations.

The exact relationship between RUNX2 and BCL11B expression is currently unclear, but bone formation in *Bcl11b*^{-/-} mice shows that RUNX2 expression is not dependent on BCL11B. In the anterior-most facial mesenchyme BCL11B is expressed independently of RUNX2. In the facial mesenchyme giving rise to the premaxillary, maxillary and palatine bones, early and late phases of BCL11B expression could be continuous, with downregulation in regions of strong RUNX2 expression, either directly by high levels of RUNX2 or by other factors. In the palatal shelf mesenchyme at E14.5, BCL11B expression is largely absent, occurring principally in RUNX2-positive cells forming the nascent palatal extension of the maxillary bones, suggesting co-regulation or RUNX2-dependence of BCL11B expression.

BCL11B has functional significance in the formation of craniofacial bone. We have shown that BCL11B expression is compatible with potential roles in the shaping of osteogenic mesenchymal condensations and/or suture formation during intramembranous ossification. Our data also suggest the potential for involvement of mutations affecting the *BCL11B* gene in human complex craniosynostosis or other craniofacial dysplasias.

3. Experimental procedures

3.1. Animals

Animal experiments were in compliance with animal welfare guidelines mandated by the Institutional Animal Care and Use Committee of the Icahn School of Medicine at Mount Sinai. Timed matings of wild-type C57BL/6J mice (Stock # 000664, The Jackson

Laboratory) were made to obtain the appropriate embryonic ages for histology and immunohistochemistry.

3.2. Histology and immunohistochemistry

Heads were fixed in 4% PFA in 1× PBS overnight at 4 °C, washed in 1× PBS, and embedded in paraffin. Three sections per slide were cut at 5 μm. Every tenth slide was stained with hematoxylin and eosin (H&E). Antibodies used were rat anti-BCL11B (1:600; Abcam, ab18465) and rabbit anti-RUNX2 (1:200; Sigma, HPA022040). Antibodies were detected by the application of Alexa Fluor 488 donkey anti-rabbit IgG (1:200; Invitrogen, A20216) or Alexa Fluor 594 goat anti-rat IgG (1:200; Invitrogen, A11007). Nuclei were stained with Hoechst 33258 (1:50,000 of a 100 mg/ml stock; Invitrogen, H1398). Alkaline phosphatase (ALP) staining was performed as described (Miao and Scutt, 2002). For each staining and structure reported, at least three mice were examined. Brightfield and fluorescent micrographs were taken on a Nikon Eclipse E600 microscope with a Nikon DXM1200 digital camera, using the NIS-Elements software program. Images were processed in Photoshop.

3.3. RNA isolation and RNA-Seq analysis

Coronal sutures, including the osteogenic fronts and intervening suture mesenchyme, were dissected by hand from E16.5 mouse embryos under a stereomicroscope, immediately frozen on dry ice, and stored at -80 °C. RNA was prepared by first homogenizing tissue in 0.5 ml of Trizol in a 1.5 ml Eppendorf tube using a Kontes Pellet Motor Pestle, adding another 0.5 ml of Trizol after homogenization, and continuing as described by the manufacturer. Resuspended RNA was DNase-digested and repurified using the RNeasy MinElute Cleanup Kit (Qiagen). Four biological replicates were prepared for RNA-Seq analysis. Each replicate consisted of the combined dissected sutures from 3 to 6 WT embryos from an individual litter.

RNA-Seq was performed by the Genetic Resources Core Facility (GRCF) at Johns Hopkins School of Medicine. Following library preparation according to the TruSeq RNA v2 Library Preparation protocol, samples were sequenced as paired-end 100 bp reads on the Illumina HiSeq 2500 platform. After adapter trimming and quality filtering, reads were mapped to the murine reference genome (NCBIM37) using Tophat (Trapnell et al., 2009). Gene expression levels were normalized and quantified using the Cufflinks package (Trapnell et al., 2010) and expressed as the number of Fragments Per Kilobase of transcript per Million mapped reads (FPKM).

Acknowledgements

The work was supported by grants, NIH/NIDCR 1 R01 DE022988 and NIH/NIDCR 1 U01 DE024448.

References

- Alcamo, E.A., Chirivella, L., Dautzenberg, M., Dobreva, G., Farinas, I., Grosschedl, R., et al., 2008. Satb2 regulates callosal projection neuron identity in the developing cerebral cortex. *Neuron* 57, 364–377.
- Arlotta, P., Molyneaux, B.J., Chen, J., Inoue, J., Kominami, R., Macklis, J.D., 2005. Neuronal subtype-specific genes that control corticospinal motor neuron development in vivo. *Neuron* 45, 207–221.
- Avram, D., Fields, A., Pretty On Top, K., Neviriv, D.J., Ishmael, J.E., Leid, M., 2000. Isolation of a novel family of C(2)H(2) zinc finger proteins implicated in transcriptional repression mediated by chicken ovalbumin upstream promoter transcription factor (COUP-TF) orphan nuclear receptors. *J. Biol. Chem.* 275, 10315–10322.
- Bradley, E.W., McGee-Lawrence, M.E., Westendorf, J.J., 2011. Hdac-mediated control of endochondral and intramembranous ossification. *Crit. Rev. Eukaryot. Gene Expr.* 21, 101–113.
- Candelierre, G.A., Liu, F., Aubin, J.E., 2001. Individual osteoblasts in the developing calvaria express different gene repertoires. *Bone* 28, 351–361.

- Chan, W., Costantino, N., Li, R., Lee, S.C., Su, Q., Melvin, D., et al., 2007. A recombineering based approach for high-throughput conditional knockout targeting vector construction. *Nucleic Acids Res.* 35, e64.
- Cherrier, T., Suzanne, S., Redel, L., Calao, M., Marban, C., Samah, B., et al., 2009. p21(WAF1) gene promoter is epigenetically silenced by CTIP2 and SUV39H1. *Oncogene* 28, 3380–3389.
- Connerney, J., Andreeva, V., Leshem, Y., Muentener, C., Mercado, M.A., Spicer, D.B., 2006. Twist1 dimer selection regulates cranial suture patterning and fusion. *Dev. Dyn.* 235, 1345–1357.
- Connerney, J., Andreeva, V., Leshem, Y., Mercado, M.A., Dowell, K., Yang, X., et al., 2008. Twist1 homodimers enhance FGF responsiveness of the cranial sutures and promote suture closure. *Dev. Biol.* 318, 323–334.
- Deckelbaum, R.A., Holmes, G., Zhao, Z., Tong, C., Basilico, C., Loomis, C.A., 2012. Regulation of cranial morphogenesis and cell fate at the neural crest-mesoderm boundary by engrailed 1. *Development* 139, 1346–1358.
- Depew, M.J., Compagnucci, C., Griffin, J., 2008. Suture neontology and paleontology: the bases for where, when and how boundaries between bones have been established and have evolved. *Front. Oral Biol.* 12, 57–78.
- Di Ieva, A., Bruner, E., Davidson, J., Pisano, P., Haider, T., Stone, S.S., et al., 2013. Cranial sutures: a multidisciplinary review. *Childs Nerv. Syst.* 29, 893–905.
- Dobreva, G., Chahrour, M., Dautzenberg, M., Chirivella, L., Kanzler, B., Farinas, I., et al., 2006. SATB2 is a multifunctional determinant of craniofacial patterning and osteoblast differentiation. *Cell* 125, 971–986.
- Golonzha, O., Leid, M., Indra, G., Indra, A.K., 2007. Expression of COUP-TF-interacting protein 2 (CTIP2) in mouse skin during development and in adulthood. *Gene Expr. Patterns* 7, 754–760.
- Golonzha, O., Liang, X., Messaddeq, N., Bornert, J.M., Campbell, A.L., Metzger, D., et al., 2009a. Dual role of COUP-TF-interacting protein 2 in epidermal homeostasis and permeability barrier formation. *J. Invest. Dermatol.* 129, 1459–1470.
- Golonzha, O., Metzger, D., Bornert, J.M., Bay, B.K., Gross, M.K., Kioussi, C., et al., 2009b. Ctip2/Bcl11b controls ameloblast formation during mammalian odontogenesis. *Proc. Natl. Acad. Sci. U.S.A.* 106, 4278–4283.
- Hall, B.K., Miyake, T., 2000. All for one and one for all: condensations and the initiation of skeletal development. *Bioessays* 22, 138–147.
- Hall, J., Jheon, A.H., Ealba, E.L., Eames, B.F., Butcher, K.D., Mak, S.S., et al., 2014. Evolution of a developmental mechanism: species-specific regulation of the cell cycle and the timing of events during craniofacial osteogenesis. *Dev. Biol.* 385, 380–395.
- Heuzé, Y., Holmes, G., Peter, I., Richtsmeier, J.T., Jabs, E.W., 2014. Closing the gap: genetic and genomic continuum from syndromic to nonsyndromic craniosynostoses. *Curr. Genet. Med. Rep.* 2, 135–145.
- Holmes, G., 2012. The role of vertebrate models in understanding craniosynostosis. *Childs Nerv. Syst.* 28, 1471–1481.
- Jabs, E.W., Lewanda, A.F., 2013. Craniosynostosis. In: Rimoin, D.L., et al. (Eds.), *Emery & Rimoin's Principles and Practice of Medical Genetics*. Churchill Livingstone, Philadelphia.
- Jiang, X., Iseki, S., Maxson, R.E., Sucov, H.M., Morrissey-Kay, G.M., 2002. Tissue origins and interactions in the mammalian skull vault. *Dev. Biol.* 241, 106–116.
- Katsuragi, Y., Anraku, J., Nakatomi, M., Ida-Yonemochi, H., Obata, M., Mishima, Y., et al., 2013. Bcl11b transcription factor plays a role in the maintenance of the ameloblast-progenitors in mouse adult maxillary incisors. *Mech. Dev.* 130, 482–492.
- Kreiborg, S., 2000. Postnatal growth and development of the craniofacial complex in premature craniosynostosis. In: Cohen, M.M., Jr., MacLean, R.E. (Eds.), *Craniosynostosis: Diagnosis, Evaluation, and Management*. Oxford University Press, New York, pp. 158–174.
- Kyrylkova, K., Kyryachenko, S., Biehs, B., Klein, O., Kioussi, C., Leid, M., 2012. BCL11B regulates epithelial proliferation and asymmetric development of the mouse mandibular incisor. *PLoS ONE* 7, e37670.
- Lana-Elola, E., Rice, R., Grigoriadis, A.E., Rice, D.P., 2007. Cell fate specification during calvarial bone and suture development. *Dev. Biol.* 311, 335–346.
- Leid, M., Ishmael, J.E., Avram, D., Shepherd, D., Fraulob, V., Dolle, P., 2004. CTIP1 and CTIP2 are differentially expressed during mouse embryogenesis. *Gene Expr. Patterns* 4, 733–739.
- Marban, C., Suzanne, S., Dequiedt, F., de Walque, S., Redel, L., Van Lint, C., et al., 2007. Recruitment of chromatin-modifying enzymes by CTIP2 promotes HIV-1 transcriptional silencing. *EMBO J.* 26, 412–423.
- Merrill, A.E., Bochukova, E.G., Brugge, S.M., Ishii, M., Pilz, D.T., Wall, S.A., et al., 2006. Cell mixing at a neural crest-mesoderm boundary and deficient ephrin-Eph signaling in the pathogenesis of craniosynostosis. *Hum. Mol. Genet.* 15, 1319–1328.
- Miao, D., Scutt, A., 2002. Histochemical localization of alkaline phosphatase activity in decalcified bone and cartilage. *J. Histochem. Cytochem.* 50, 333–340.
- Miller, E.S., Berman, S.D., Yuan, T.L., Lees, J.A., 2010. Disruption of calvarial ossification in E2f4 mutant embryos correlates with increased proliferation and progenitor cell populations. *Cell Cycle* 9, 2620–2628.
- Morrissey-Kay, G.M., Wilkie, A.O., 2005. Growth of the normal skull vault and its alteration in craniosynostosis: insights from human genetics and experimental studies. *J. Anat.* 207, 637–653.
- Opperman, L.A., 2000. Cranial sutures as intramembranous bone growth sites. *Dev. Dyn.* 219, 472–485.
- Senawong, T., Peterson, V.J., Avram, D., Shepherd, D.M., Frye, R.A., Minucci, S., et al., 2003. Involvement of the histone deacetylase SIRT1 in chicken ovalbumin upstream promoter transcription factor (COUP-TF)-interacting protein 2-mediated transcriptional repression. *J. Biol. Chem.* 278, 43041–43050.
- Sharma, V.P., Fenwick, A.L., Brockop, M.S., McGowan, S.J., Goos, J.A., Hoogeboom, A.J., et al., 2013. Mutations in TCF12, encoding a basic helix-loop-helix partner of TWIST1, are a frequent cause of coronal craniosynostosis. *Nat. Genet.* 45, 304–307.
- Szemes, M., Gyorgy, A., Pawelez, C., Dobi, A., Agoston, D.V., 2006. Isolation and characterization of SATB2, a novel AT-rich DNA binding protein expressed in development- and cell-specific manner in the rat brain. *Neurochem. Res.* 31, 237–246.
- Ting, M.C., Wu, N.L., Roybal, P.G., Sun, J., Liu, L., Yen, Y., et al., 2009. EphA4 as an effector of Twist1 in the guidance of osteogenic precursor cells during calvarial bone growth and in craniosynostosis. *Development* 136, 855–864.
- Topark-Ngarm, A., Golonzha, O., Peterson, V.J., Barrett, B., Jr., Martinez, B., Crofoot, K., et al., 2006. CTIP2 associates with the NuRD complex on the promoter of p57KIP2, a newly identified CTIP2 target gene. *J. Biol. Chem.* 281, 32272–32283.
- Trapnell, C., Pachter, L., Salzberg, S.L., 2009. TopHat: discovering splice junctions with RNA-Seq. *Bioinformatics* 25, 1105–1111.
- Trapnell, C., Williams, B.A., Pertea, G., Mortazavi, A., Kwan, G., van Baren, M.J., et al., 2010. Transcript assembly and quantification by RNA-Seq reveals unannotated transcripts and isoform switching during cell differentiation. *Nat. Biotechnol.* 28, 511–515.
- Wakabayashi, Y., Watanabe, H., Inoue, J., Takeda, N., Sakata, J., Mishima, Y., et al., 2003. Bcl11b is required for differentiation and survival of alphabeta T lymphocytes. *Nat. Immunol.* 4, 533–539.
- Wilkie, A.O., Byren, J.C., Hurst, J.A., Jayamohan, J., Johnson, D., Knight, S.J., et al., 2010. Prevalence and complications of single-gene and chromosomal disorders in craniosynostosis. *Pediatrics* 126, 391–400.
- Yen, H.Y., Ting, M.C., Maxson, R.E., 2010. Jagged1 functions downstream of Twist1 in the specification of the coronal suture and the formation of a boundary between osteogenic and non-osteogenic cells. *Dev. Biol.* 347, 258–270.
- Yoshida, T., Vivatbuttsiri, P., Morrissey-Kay, G., Saga, Y., Iseki, S., 2008. Cell lineage in mammalian craniofacial mesenchyme. *Mech. Dev.* 125, 797–808.
- Zhang, L.J., Bhattacharya, S., Leid, M., Ganguli-Indra, G., Indra, A.K., 2012. Ctip2 is a dynamic regulator of epidermal proliferation and differentiation by integrating EGFR and Notch signaling. *J. Cell Sci.* 125, 5733–5744.